ACS Catalysis

Letter

pubs.acs.org/acscatalysis

CO_2 Reduction to Methanol on TiO_2-Passivated GaP Photocatalysts

Guangtong Zeng,[†] Jing Qiu,[‡] Zhen Li,[§] Prathamesh Pavaskar,[§] and Stephen B. Cronin*[,†,§]

[†]Department of Chemistry, [‡]Department of Materials Science, and [§]Department of Electrical Engineering, University of Southern California, Los Angeles, California 90089, United States

Supporting Information

ABSTRACT: In the past, the electrochemical instability of III−V semiconductors has severely limited their applicability in photocatlaysis. As a result, a vast majority of the research on photocatalysis has been done on TiO_2, which is chemically robust over a wide range of pH. However, TiO_2 has a wide band gap (3.2 eV) and can only absorb ∼4% of the solar spectrum, and thus, it will never provide efficient solar energy conversion/storage on its own. Here, we report photocatalytic CO_2 reduction with water to produce methanol using TiO_2-passivated GaP photocathodes under 532 nm wavelength illumination. The TiO_2 layer prevents corrosion of the GaP, as evidenced by atomic force microscopy and photoelectrochemical measurements. Here, the GaP surface is passivated using a thin film of TiO_2 deposited by atomic layer deposition (ALD), which provides a viable, stable photocatalyst without sacrificing photocatalytic efficiency. In addition to providing a stable photocatalytic surface, the TiO_2 passivation provides substantial enhancement in the photoconversion efficiency through passivation of surface states, which cause nonradiative carrier recombination. In addition to passivation effects, the TiO_2 deposited by ALD is n-type due to oxygen vacancies and forms a pn-junction with the underlying p-type GaP photocathode. This creates a built-in field that assists in the separation of photogenerated electron−hole pairs, further reducing recombination. This reduction in the surface recombination velocity (SRV) corresponds to a shift in the overpotential of almost 0.5 V. No enhancement is observed for TiO_2 thicknesses above 10 nm, due to the insulating nature of the TiO_2, which eventually outweighs the benefits of passivation.

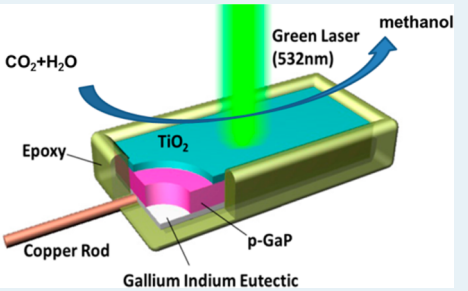

KEYWORDS: *photoelectrochemical, GaP, CO_2 reduction, TiO_2 passivated, methanol*

The photoelectrochemical reduction of CO_2 is an exciting reaction system with the ability to convert an abundant greenhouse gas to combustible hydrocarbon fuels using sunlight. The direct conversion of solar-to-chemical energy has several advantages over solar-to-electric energy conversion, most notably, the ability to store large amounts of energy (∼GW) in chemical bonds that can later be released in a carbon neutral cycle.[1] Many attempts have been made to reduce CO_2 by $2e^-$ to various species such as CO and formic acid, as reported in previous literature.[2] Few researchers have achieved further reduction to CH_3OH or CH_4.[3] Methanol is an attractive product with a relatively high energy density, which can be easily integrated into the existing liquid fuel technologies.[1g,4] However, the photocatalytic reduction of CO_2 with H_2O to methanol requires six electrons and many intermediate species, some of which have extremely high energy barriers.[5] The most likely first step in this multielectron reaction is the one electron reduction to the CO_2^- intermediate,[6] which lies 1.7 eV above the conduction band of TiO_2 and 1.2 eV above GaP. The mechanism for electrochemical CO_2 reduction was first proposed by Bockris et al.[7] The high overpotential required for this reaction was attributed to the formation of the CO_2^- intermediate, which consequently converts to CO via the general process $CO_2 + e^- \rightarrow CO_2^-$, $CO_2^- + 2H^+ + e^- \rightarrow CO + H_2O$.[1c,i,3a,8] In 1978, Hallman's group first reported CO_2 reduction on p-GaP under 365 nm illumination with an applied overpotential of −1.4 V (vs SCE).[2a] Fujishima and Honda demonstrated photoelectrocatalytic reduction of CO_2 to formaldehyde and methanol by irradiating TiO_2 and GaP with the UV light at an overpotential of −1.5 V (vs SCE).[2b,9] Canfield later reported CO_2 reduction to methanol on p-InP with an overpotential of −1.3 V (vs SCE).[2h] More recently, Bocarsly's group demonstrated pyridinium-catalyzed CO_2 reduction on GaP photocathodes with overpotentials between −0.7 V and −0.2 V (vs SCE) under UV light.[3a] Despite these interesting prior results, the stability of these materials against photocorrosion has not been addressed.

In the work presented here, we investigate the photocatalytic performance and stability of TiO_2-passivated p-GaP using atomic force microscopy (AFM), photoelectrochemistry, and optical microscopy. The photocatalytic efficiency is studied systematically as a function of TiO_2 layer thickness using a three-terminal potentiostat. The products are detected using NMR spectroscopy and gas chromatography, systematically as a function of applied overpotential.

Zn doped p-type (100) oriented GaP with a dopant concentration of 2×10^{18} cm^{-3} was used as the photocatalyst for CO_2 reduction with an active area of 0.5 cm × 1 cm. Atomic layer deposition (ALD) of anatase TiO_2 was performed at 250 °C on the p-GaP wafers with $TiCl_4$ as the titanium source and

Received: March 11, 2014
Revised: August 21, 2014

   dx.doi.org/10.1021/cs500697w | ACS Catal. XXXX, XXX, XXX−XXX

water vapor as the oxygen source. The antase crystal phase was verified by Raman spectroscopy. Using ellipsometry, we established that 100 cycles of ALD produces a 4 nm thick TiO_2 film and 1000 cycles produces a 40 nm film. A Ga−In eutectic film was painted on the back of the p-GaP to form an Ohmic contact. The Ga−In contact was then connected to the external circuitry with a copper wire and coated with epoxy cement to insulate it from the electrolytic solution, as illustrated in Figure 1b. Although this planar geometry is not ideal for high

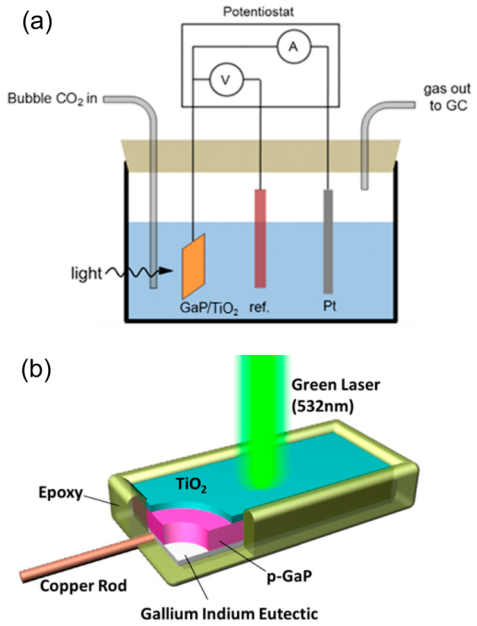

Figure 1. Schematic diagram of (a) photoelectrochemical measurement setup and (b) sample geometry of the TiO_2-passivated p-GaP photocathode.

efficiency photoconversion, it enables us to study surface stability. A three-terminal potentiostat was used with the prepared semiconductor samples as the working electrode, a Ag/AgCl electrode as the reference electrode, and a Pt electrode functioning as a counter electrode, as shown in Figure 1a. The photocatalytic reaction rates of two sets of samples were measured in a 2 mL solution of 0.5 M NaCl, with and without 10 mM pyridine, while continuously bubbling CO_2 through the solution. NaCl (0.5 M) was chosen as the electrolyte solution because of its high conductance and its ability to stabilize the intermediate states involved in the CO_2 reduction.[10] In this setup, we analyze the products evolving at the working electrode, instead of at the counter electrode. It is likely that oxygen is also produced in the reaction.

While photocatalysis on GaP (and other III−V compound semiconductors) has been demonstrated previously,[2h,3a,11] this material corrodes rapidly under photoelectrochemical conditions and is significantly degraded after just 30 min of illumination. In order to make GaP photochemically stable, we passivated the surface using a thin film of TiO_2 deposited by ALD, as illustrated schematically in Figure 1b. Figure 2a,b show optical microscope and atomic force microscope images of the bare GaP surface after 8 h of illumination. Figure 2c shows a plot of the surface topography obtained along the dashed white line in Figure 2b, showing an RMS roughness of ±54 nm, which indicates that substantial photocorrosion has taken place and that this will not serve as a viable photocatalyst. In contrast, the photocurrent density of TiO_2-passivated GaP is stable for 8 h. The optical microscope image (Figure 2d) and atomic force microscope image (Figure 2e) exhibit no evidence of surface corrosion or damage after 8 h, with an RMS roughness of ±1 nm (Figure 2f), indicating that this is a long-term, stable photocatalyst. Here, the TiO_2 significantly improves the photostablilty of the GaP surface, however, more extensive time-dependent studies are needed in order to establish the extent of this long-term stability.

In addition to providing a stable photocatalytic surface, the TiO_2 passivation layer results in an increase in the photoconversion efficiency. Figure 3a shows the photocurrent−voltage curves for GaP passivated with various thicknesses of TiO_2 measured in a 0.5 M NaCl, 10 mM pyridine solution under 532 nm illumination. During these measurements, CO_2 is continuously bubbled through the solution. Bare GaP (green curve) has an onset of photocurrent at a potential of approximately −0.15 V (vs NHE). For TiO_2-passivated GaP, we see a clear shift in the overpotential required to drive this reaction with increasing thickness of the TiO_2, as plotted in Figure 3b. Table 1 lists the shift of onset overpotential of samples with different thicknesses of TiO_2. For example, the onset potential for 10 nm TiO_2 (red curve) is shifted by 0.5 V with respect to bare GaP. This shift is attributed to the passivation of surface states that cause nonradiative recombination and the formation of a pn-junction, which is created because the ALD-deposited TiO_2 tends to be n-type doped due to oxygen vacancies.[12] Figure 3c shows the built-in potential for the junction calculated using $V_{bi} = (((W_D^2\, q)/(2\, \epsilon_0\, \epsilon_a\, \epsilon_d))\ (N_a\, N_d(N_a\ \epsilon_a\ +\ N_d\ \epsilon_d)/(N_a\ +\ N_d)^2))$, assuming a doping concentration of $N_a = 5 \times 10^{18}$cm^3.[13] Here, W_D is the depletion width of the GaP−TiO_2 junction, which is a function of the TiO_2 layer thickness. This simple calculation predicts values similar to the experimentally observed shift in the overpotential plotted in Figure 3b. Beyond 10 nm, however, the photocurrent decreases rapidly with increasing TiO_2 thickness due to band bending at the n-type TiO_2/electrolyte interface, which blocks electrons. No enhancement is observed for TiO_2 thicknesses above 10 nm, due to the insulating nature of the TiO_2, which eventually outweighs the benefits of passivation. Although TiO_2 does not absorb light at 532 nm, the pn-junction formed with the GaP enables separation of the photogenerated charge in the actively absorbing GaP. Figure 3d shows the NMR spectra taken after 8 h of illumination with an overpotential of −0.50 V vs NHE for GaP with and without TiO_2 passivation. These data show a clear peak corresponding to methanol, as reported previously by Barton et al.[3a] Gas chromatography FID data have also been used to verify the production of methanol, as shown in Supporting Information Figure S1. On the basis of these GC FID data for the 5 nm thick TiO_2 sample, we calculated that 4.9 (±0.02) μmol of CH_3OH are produced during an 8 h reaction consuming 5.2 Coulombs of charge. Dividing by this ratio by the stoichiometric factor of 6, yields a Faradaic efficiency of 55%. Also, according to the GC TCD data of the same experiment, H_2 is produced with a Faradaic efficiency of 30%. The photoconversion efficiency, however, can be significantly less than this due to nonradiative recombination, which is unknown, particularly for this planar sample geometry. As a control experiment, the same reaction was run under the same electrochemical conditions of −0.50 V vs NHE without laser illumination, which resulted in no measurable current and no detectable methanol in the NMR spectra. In order to rule out

dx.doi.org/10.1021/cs500697w | ACS Catal. XXXX, XXX, XXX−XXX

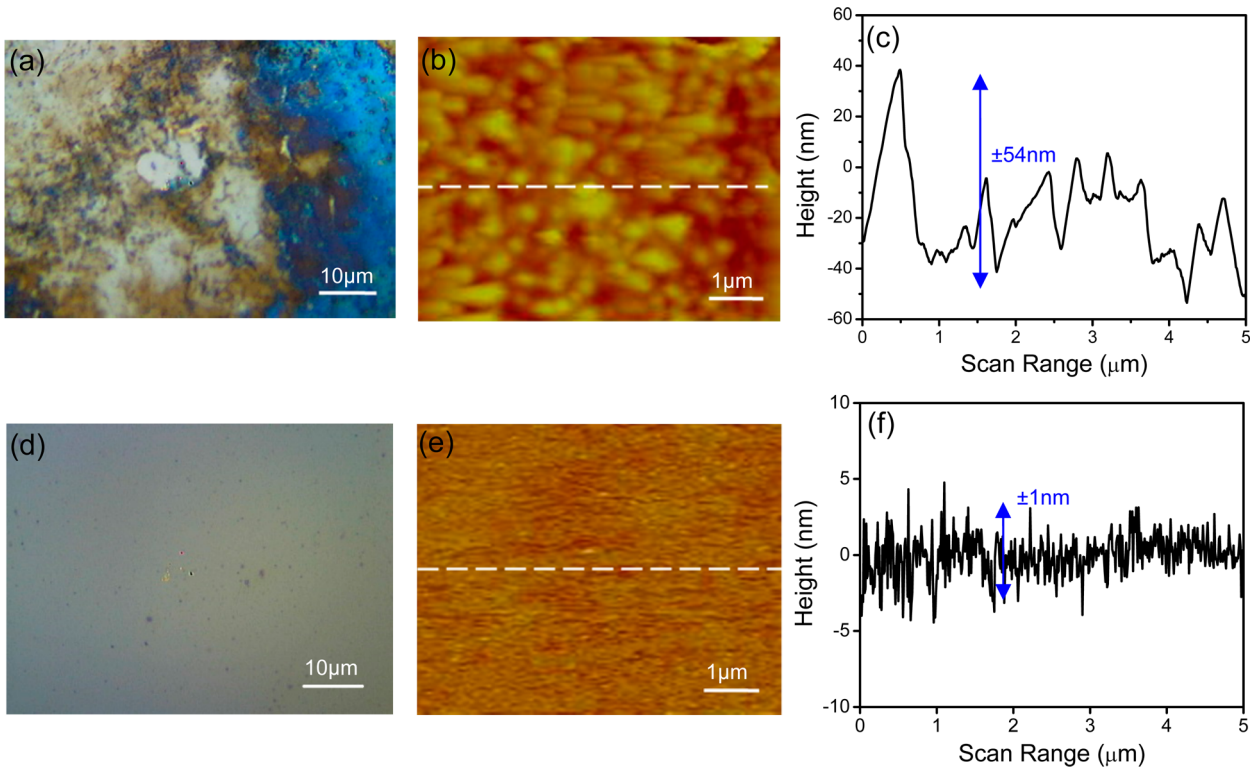

Figure 2. (a) Optical microscope image, (b) atomic force microscope image, and (c) surface topography of bare GaP surface after an 8 h reaction at −0.5 V overpotential. (d) Optical microscope image, (e) atomic force microscope image, and (f) surface topography of 5 nm TiO_2 on GaP surface after an 8 h reaction.

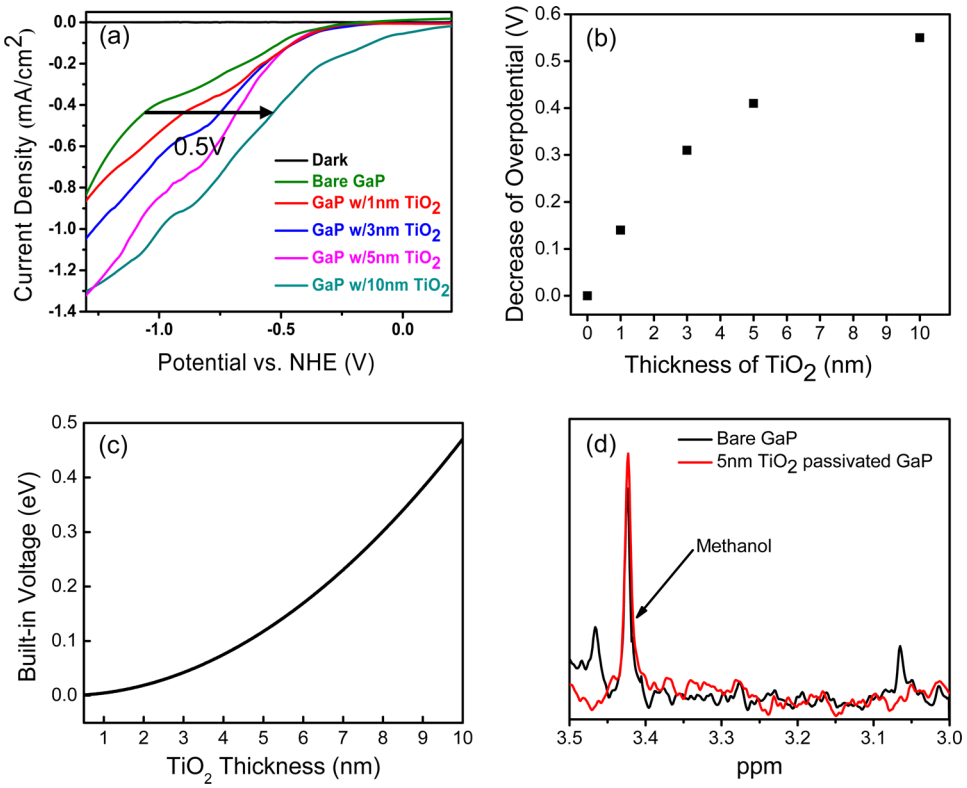

Figure 3. (a) Photocatalytic current−potential curves of GaP photocatalysts with different TiO_2 thicknesses in a 0.5 M NaCl, 10 mM pyridine solution under 532 nm wavelength laser illumination. (b) Decrease of overpotential plotted as a function of TiO_2 thickness on GaP. (c) Calculated built-in voltage plotted as a function of TiO_2 thickness. (d) NMR spectra showing methanol production using bare GaP and 5 nm TiO_2-passiavated GaP photocatalysts at an overpotential of −0.50 V.

dx.doi.org/10.1021/cs500697w | ACS Catal. XXXX, XXX, XXX−XXX

Table 1. Shift of Onset Overpotential for Samples with Different Thicknesses of TiO_2

catalysts	shift of onset overpotential compared to bare GaP (V)
bare GaP	0
1 nm TiO_2@GaP	0.13
3 nm TiO_2@GaP	0.31
5 nm TiO_2@GaP	0.40
10 nm TiO_2@GaP	0.52

other sources of carbon in this reaction, we used isotopically labeled $^{13}CO_2$ as the carbon source in this reaction and observed $^{13}CH_3OH$ in the ^{13}C NMR spectrum shown in Supporting Information Figure S5.[14] In addition, we repeated the experiment, purging with Ar instead of CO_2, and found no production of hydrocarbons. Therefore, we are confident that CO_2 is the only carbon source in this reaction. Previously, it was reported that a pyridine catalyst is required to drive this reaction on GaP. The pyridinium radical serves as a one-electron charge-transfer mediator, which is capable of efficiently transferring all six electrons to reduce CO_2 to methanol, thereby circumventing the high energy barrier of the one-electron reduction of CO_2 mentioned above.[11] However, we observe the same methanol peak in our NMR spectra without pyridine in solution (see Supporting Information Figure S2), indicating that this catalyst is not, in fact, required to drive this reaction at low overpotentials. Although CH_3OH products are observed without pyridine, the yield is one-third that of the system with pyridine, indicating that the pyridine, in fact, helps lower the energy barriers of the reaction by forming an inner-sphere-type electron-transfer system.[11,15] Atomic force microscopy shows that the GaP/TiO_2 is photochemically stable without pyridine, as shown in Supporting Information Figure S3.

In order to understand the mechanism of this reaction, we must consider the energetics of the electrons in this photocatalytic structure. The conduction bands of GaP and TiO_2 lie slightly above NHE at −0.7 V and −0.2 V versus NHE, respectively, as plotted in Figure 4. This leaves an energy barrier of at least 1.2 V for the electrons to overcome in the reduction of CO_2. The −0.5 V externally applied overpotential (V_{ext}) accounts for part of this required energy, and the photovoltage produced at the internal pn-junction and/or the liquid-semiconductor junction (V_{PV}) can easily account for the remaining −0.7 V, as depicted in Figure 4. From the flat-band voltage, we can obtain the open circuit voltage, as follows: $(V_{oc})_{max} = |V_{fb} - V_{redox}|$, where V_{fb} is flat-band potential and V_{redox} is the potential of the redox couple.[16] From Mott−Schottky measurements, we obtained a flat-band potential of 0.4 V versus NHE, which is consistent with previous values from literature.[3a,17] Using V_{redox} (ferricyanide/ferroyanide) = 0.36 V, we obtain an open circuit voltage of V_{oc} = 0.76 V, which is large enough to cover the remaining −0.7 V depicted in Figure 4. This photovoltage is reasonable considering GaP's relatively large band gap of 2.25 eV.

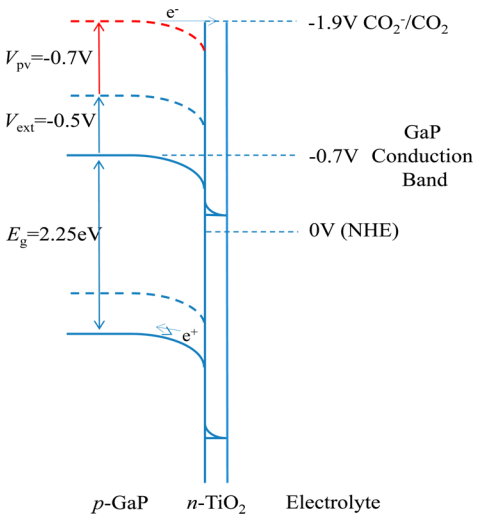

Figure 4. Energy band alignment of GaP and TiO_2 together with the relevant redox potentials of CO_2.

These estimations assume that the electrons traverse the TiO_2 layer ballistically and do not equilibrate to the TiO_2 conduction band edge. In the diffusive case, an additional 0.5 V would be required. We believe this is one of the reasons why the TiO_2 layer must be made very thin. Several aspects of these results and their underlying mechanism are quite surprising. First, we had initially thought that the TiO_2 layer, which is insulating and has a low conduction band energy, would lower the overall photocatalytic efficiency (i.e., photocurrent), but would, at least, provide a stable, viable catalyst. Much to our surprise, the TiO_2 layer actually improved the overall photoconversion efficiency. The reasons for this are 3-fold: (1) The TiO_2 reduces nonradiative recombination of the photoexcited electron−hole pairs. (2) The electrons traverse the TiO_2 ballistically and, therefore, do not relax to the conduction band edge. (3) The formation of a pn-junction provides an additional photovoltage required to drive the reaction.

It is important to note, however, that the CO_2^- reduction potential of −1.9 V versus NHE is calculated from simple thermodynamic considerations for isolated CO_2^- species, and does not include the effects of the solution or catalytic surface. As a result, the energetics of the actual CO_2^- intermediates can be quite different due to the presence of the aqueous solution and/or the catalytic surface. In a mechanism proposed by Anpo et al., the CO_2^- intermediate is strongly bound to a proposed Ti^{3+} active site (oxygen vacancy) on the TiO_2 surface, thus lowering its energy.[18] Another strategy for lowering the reaction barrier is stabilizing the CO_2^- intermediate, which was recently demonstrated using an ionic liquid electrolyte cocatalyst where the cation forms a complex with the anionic intermediate.[19] Two-electron processes have also been proposed by Tananka et al., which would circumvent this first intermediate step altogether.[20] Although several mechanisms have been proposed in the literature, further spectroscopic studies are needed in order to verify the catalytic reaction pathway.

In conclusion, we report photocatalytic CO_2 reduction on TiO_2-passivated GaP. The TiO_2 passivation layer successfully stabilizes the GaP surface in solution, preventing it from photocorrosion. In addition, the TiO_2 passivation layer provides enhancement in the photoconversion efficiency through the passivation of surface states and the formation of a charge separating pn-region, which reduces carrier recombination and lowers the overpotential required to initiate this reaction by approximately 0.5 V. This general approach of passivating narrower band gap semiconductors with TiO_2 will enable more efficient photocatalysts to be developed and a broad range of materials to be considered for photocatalysis

dx.doi.org/10.1021/cs500697w | ACS Catal. XXXX, XXX, XXX−XXX

that make more efficient use of the solar spectrum. We also observe CH_3OH evolution with and without pyridine catalyst, indicating that this catalysts is not, in fact, required to drive this reaction at low overpotentials.

■ ASSOCIATED CONTENT

Supporting Information

Gas chromatography data; ^1H NMR spectra of methanol; images using optical microscopy, atomic force microscopy, and surface topography, CH_3OH production plotted as a function of time; and 13C NMR spectrum of methanol. This material is available free of charge via the Internet at http://pubs.acs.org.

■ AUTHOR INFORMATION

Corresponding Author

*E-mail: scronin@usc.edu.

Notes

The authors declare no competing financial interest.

■ ACKNOWLEDGMENTS

This research was supported by ONR Award No. N00014-12-1-0570 (J.Q.) and NSF Award No. CBET-0854118 (G.Z.).

■ REFERENCES

(1) (a) Benson, E. E.; Kubiak, C. P.; Sathrum, A. J.; Smieja, J. M. *Chem. Soc. Rev.* **2009**, *38* (1), 89−99. (b) Kumar, B.; Llorente, M.; Froehlich, J.; Dang, T.; Sathrum, A.; Kubiak, C. P. *Annu. Rev. Phys. Chem.* **2012**, *63*, 541−569. (c) Amatore, C.; Saveant, J. M. *J. Am. Chem. Soc.* **1981**, *103* (17), 5021−5023. (d) Cokoja, M.; Bruckmeier, C.; Rieger, B.; Herrmann, W. A.; Kühn, F. E. *Angew. Chem., Int. Ed.* **2011**, *50* (37), 8510−8537. (e) Finn, C.; Schnittger, S.; Yellowlees, L. J.; Love, J. B. *Chem. Commun.* **2012**, *48* (10), 1392−1399. (f) Goeppert, A.; Czaun, M.; May, R. B.; Prakash, G. K. S.; Olah, G. A.; Narayanan, S. R. *J. Am. Chem. Soc.* **2011**, *133* (50), 20164−20167. (g) Olah, G. A.; Prakash, G. K. S.; Goeppert, A. *J. Am. Chem. Soc.* **2011**, *133* (33), 12881−12898. (h) Le, M.; Ren, M.; Zhang, Z.; Sprunger, P. T.; Kurtz, R. L.; Flake, J. C. *J. Electrochem. Soc.* **2011**, *158* (5), E45−E49. (i) Bard, A. J.; Faulkner, L. R. *Electrochemical Methods: Fundamentals and Applications*, 2nd ed.; John Wiley & Sons, Inc: New York, 2001. (j) Izumi, Y. *Coord. Chem. Rev.* **2013**, *257* (1), 171−186. (k) Varghese, O. K.; Paulose, M.; LaTempa, T. J.; Grimes, C. A. *Nano Lett.* **2009**, *9* (2), 731−737.

(2) (a) Halmann, M. *Nature* **1978**, *275* (5676), 115−116. (b) Inoue, T.; Fujishima, A.; Konishi, S.; Honda, K. *Nature* **1979**, *277*, 637−638. (c) Chen, Z.; Chen, C.; Weinberg, D. R.; Kang, P.; Concepcion, J. J.; Harrison, D. P.; Brookhart, M. S.; Meyer, T. J. *Chem. Commun.* **2011**, *47* (47), 12607−12609. (d) Morris, A. J.; Meyer, G. J.; Fujita, E. *Acc. Chem. Res.* **2009**, *42* (12), 1983−1994. (e) Jacquet, O.; Frogneux, X.; Das Neves Gomes, C.; Cantat, T. *Chem. Sci.* **2013**, *4* (5), 2127−2131. (f) Costentin, C.; Drouet, S.; Robert, M.; Savéant, J.-M. *Science* **2012**, *338* (6103), 90−94. (g) Costentin, C.; Canales, J. C.; Haddou, B.; Savéant, J.-M. *J. Am. Chem. Soc.* **2013**, *135* (47), 17671−17674. (h) Canfield, D.; Frese, K. W. *J. Electrochem. Soc.* **1983**, *130* (8), 1772−1773.

(3) (a) Barton, E. E.; Rampulla, D. M.; Bocarsly, A. B. *J. Am. Chem. Soc.* **2008**, *130* (20), 6342−6344. (b) Doherty, M. D.; Grills, D. C.; Muckerman, J. T.; Polyansky, D. E.; Fujita, E. *Coord. Chem. Rev.* **2010**, *254* (21−22), 2472−2482. (c) Savéant, J.-M. *Chem. Rev.* **2008**, *108* (7), 2348−2378.

(4) Olah, G. A.; Goeppert, A.; Prakash, G. K. S. *J. Org. Chem.* **2008**, *74* (2), 487−498.

(5) Kumar, B.; Llorente, M.; Froehlich, J.; Dang, T.; Sathrum, A.; Kubiak, C. P. *Annu. Rev. Phys. Chem.* **2012**, *63*, 541−569.

(6) Taniguchi, I.; Aurian-Blajeni, B.; Bockris, J. O. M. *Electrochim. Acta* **1984**, *29* (7), 923−932.

(7) (a) Chandrasekaran, K.; Bockris, J. O. *Surf. Sci.* **1987**, *185* (3), 495−514. (b) Bockris, J. O.; Wass, J. C. *J. Electrochem. Soc.* **1989**, *136* (9), 2521−2528. (c) Bockris, J. O.; Wass, J. C. *Mater. Chem. Phys.* **1989**, *22* (3−4), 249−280.

(8) Seshadri, G.; Lin, C.; Bocarsly, A. B. *J. Electroanal. Chem.* **1994**, *372* (1−2), 145−150.

(9) Inoue, T.; Fujishima, A.; Konishi, S.; Honda, K. *Nature* **1979**, *277*, 637.

(10) Boston, D. J.; Xu, C.; Armstrong, D. W.; MacDonnell, F. M. *J. Am. Chem. Soc.* **2013**, *135* (44), 16252−16255.

(11) Barton Cole, E.; Lakkaraju, P. S.; Rampulla, D. M.; Morris, A. J.; Abelev, E.; Bocarsly, A. B. *J. Am. Chem. Soc.* **2010**, *132* (33), 11539−11551.

(12) (a) Morgan, B. J.; Watson, G. W. *J. Phys. Chem. C* **2010**, *114* (5), 2321−2328. (b) Qiu, J.; Zeng, G.; Pavaskar, P.; Li, Z.; Cronin, S. B. *Phys. Chem. Chem. Phys.* **2014**, *16* (7), 3115−3121.

(13) Neamen, D. A. *Semiconductor Physics and Devices*, 3rd ed.; McGraw-Hill: New York, 2003; pp 241−265.

(14) Fulmer, G. R.; Miller, A. J. M.; Sherden, N. H.; Gottlieb, H. E.; Nudelman, A.; Stoltz, B. M.; Bercaw, J. E.; Goldberg, K. I. *Organometallics* **2010**, *29* (9), 2176−2179.

(15) Yan, Y.; Zeitler, E. L.; Gu, J.; Hu, Y.; Bocarsly, A. B. *J. Am. Chem. Soc.* **2013**, *135* (38), 14020−14023.

(16) Bard, A. J.; Bocarsly, A. B.; Fan, F. R. F.; Walton, E. G.; Wrighton, M. S. *J. Am. Chem. Soc.* **1980**, *102* (11), 3671−3677.

(17) Grätzel, M. *Nature* **2001**, *414* (6861), 338−344.

(18) Anpo, M.; Yamashita, H.; Ichihashi, Y.; Ehara, S. *J. Electroanal. Chem.* **1995**, *396* (1−2), 21−26.

(19) Rosen, B. A.; Salehi-Khojin, A.; Thorson, M. R.; Zhu, W.; Whipple, D. T.; Kenis, P. J. A.; Masel, R. I. *Science* **2011**, *334* (6056), 643−644.

(20) Tanaka, K.; Miyahara, K.; Toyoshima, I. *J. Phys. Chem.* **1984**, *88* (16), 3504−3508.